Highlights

- The biological activity of selected essential oil components against strains of *E. coli* and *S. aureus* are presented.
- Structure-activity relationships are derived from minimum inhibitory concentration data and propose important molecular descriptors in essential oil biological activity.
- Molecular topography of the components, electrostatic nature and ligand efficiency of the components are highlighted as principal descriptors

Title: Structure-Activity Modelling of Essential Oils, their Components, and Key Molecular Parameters and Descriptors.

Lucy Owen[a], Katie Laird[a] and Philippe B. Wilson[b].

[a] Infectious Disease Research Group, The School of Pharmacy, De Montfort University, Leicester, UK.

[b]The School of Pharmacy, De Montfort University, Leicester, UK.

Corresponding Author: Philippe B. Wilson, The School of Pharmacy, De Montfort University, Leicester, UK, philippe.wilson@dmu.ac.uk**.**

Abstract

Many essential oil components are known to possess broad spectrum antimicrobial activity, including against antibiotic resistant bacteria. These compounds may be a useful source of new and novel antimicrobials. However, there is limited research on the structure-activity relationship (SAR) of essential oil compounds, which is important for target identification and lead optimization. This study aimed to elucidate SARs of essential oil components from experimental and literature sources. Minimum Inhibitory Concentrations (MICs) of essential oil components were determined against *Escherichia coli and Staphylococcus aureus* using a microdilution method and then compared to those in published in literature. Of 12 essential oil components tested, carvacrol and cuminaldehyde were most potent with MICs of 1.98 and 2.10 mM, respectively. The activity of 21 compounds obtained from the literature, MICs ranged from 0.004 mM for limonene to 36.18 mM for α-terpineol. A 3D qualitative SAR model was generated from MICs using FORGE software by consideration of electrostatic and steric parameters. An r^2 value of 0.807 for training and cross-validation sets was achieved with the model developed. Ligand efficiency was found to correlate well to the observed activity (r^2=0.792), while strongly negative electrostatic regions were present in potent molecules. These descriptors may be useful for target identification ofessential oils or their major components in antimicrobial/drug development .

Keywords: Essential oil, antimicrobial, structure-activity relationship, *Escherichia coli, Staphylococcus aureus.*

1. Introduction

Antimicrobial resistance has greatly increased in recent years and is now considered a global public health threat [1]. Novel antimicrobials are needed to continue treating antibiotic resistant infections, yet the production of new antibiotics has stalled [2]. Natural products are a reservoir of structurally diverse compounds, so may be a source for the development of novel antimicrobial agents. Essential Oils (EOs) have been the subject of scientific interest over recent decades, with extensive screening

indicating that many of these plant extracts and their isolated components possess antimicrobial activity [3].

EOs are aromatic, oily plant extracts derived by steam distillation. They are complex mixture of volatile, low molecular weight organic compounds [4]. Terpenes and their oxygenated derivatives, terpenoids, are the most common EO compounds [5], while phenylpropanoids and benzenoid compounds are less abundant [6]. Numerous EO components inhibit an array of clinically relevant pathogenic bacteria, including antibiotic resistant isolates, suggesting they may be candidates for the development of new antimicrobials. For example, carvacrol, thymol and menthol inhibited 11 important foodborne pathogens at MICs ranging 0.02-4.0 µg/mL [7]. The EO compounds 1,8-cineole, carvacrol, terpinen-4-ol, eugenol and cinnamaldehyde inhibited *Staphylococcus aureus* and Methicillin Resistant *S. aureus* (MRSA) at Minimum Inhibitory Concentrations (MICs) ranging 0.006 to 1.6% and *Enterococcus faecalis* at MICs ranging 0.012 to >3.2% [8]. Wang et al. [9] reported that hinokitiol inhibited MRSA and *Escherichia coli* at 60 and 40 µg/ml, respectively. Orhan et al. [10] showed that thirty-five EO components inhibited 11 isolates of *Klebsiella pneumoniae,* including extended-spectrum beta-lactamase producing strains, at MICs ranging 8-64 µg/mL.

The mechanism by which EO components exert their antimicrobial effect is incompletely understood. Much of the published research has concluded that EO components change the structure and function of bacterial cell membranes; it has been proposed that the hydrophobic nature of these compounds allows them to partition in the membrane [11]. This non-specific mechanism of action is assumed to bypass many antibiotic resistance mechanisms and inhibit antibiotic resistant isolates. Moreover, it has been hypothesised that the risk of antibiotic resistance developing is lower than other antibiotics [12], as per other membrane-targeting antimicrobials such as cationic antimicrobial peptides [13]. EO components could be an attractive class of compounds for the development of new antimicrobial therapies.

Understanding the Structure-Activity Relationships (SAR) of antimicrobial agents is important in antimicrobial development to identify the most potent compounds and allow optimization of lead compounds, however there are limited published studies on the SAR of EO components as

antimicrobial agents. The hydrophobicity of EO components, measured by octanal/water partitioning coefficient (log *P*) has been correlated with their antimicrobial activity [14,15]. For example, Ben Arfa et al. [15] reported that carvacrol (log *P* = 3.52) was more antimicrobial than eugenol (log*P* = 2.73). The positive correlation of hydrophobicity and antimicrobial activity relates to a greater affinity for partitioning in the bacterial cell membrane, this correlation does not hold true at log*P* greater than 4, indicating that there are other important structural characteristics [15,16]

Several published papers have emphasised the role of a phenolic group in activity, for example, Andrade-Ochoa et al. [14] reported that thymol, which possesses a phenolic group had a significantly lower MIC than menthol, which has the equivalent structure but is alicyclic. The importance of a hydroxyl moiety alongside a phenolic group was demonstrated by comparing with aromatic compounds with alkyl substituents [14,16,17]. It is hypothesised that the delocalised electron system of the phenolic moiety facilitates proton exchange through the hydroxyl group, which dissipates proton motive force [16].

This study aims to construct a 3D QSAR model of EO component activity from experimental and literature sources based on electrostatic and steric descriptors to inform future antimicrobial drug target identification.

2. Materials and Methods

2.1. EO Components

Authentic standards of (-)-β-pinene (99%), carvacrol (98%), cuminaldehyde (98%), linalool (97%), p-cymene (99%), thymol (≥98.5%), β-caryophyllene (≥80%) and γ-terpinene (97%) were obtained from Sigma Aldrich (Gillingham, UK).

2.2. Microorganisms

Escherichia coli NCTC 8003 and *Staphylococcus aureus* NCTC 12981 were cultured using nutrient broth and agar (Oxoid, Basingstoke, UK) and grown aerobically at 37˚C for 24 hours.

2.3. Minimum Inhibitory Concentrations

The MIC of EO components were determined using a broth microdilution method adapted from the International Organization for Standardisation (ISO) 20776-1 antibiotic susceptibility test [18]. Serial two-fold dilutions of EO components to yield final concentrations ranging 8-0.01% (v/v) in nutrient broth supplemented with 10% dimethyl sulfoxide (Fisher Scientific, Loughborough, UK) were prepared in polystyrene 96-well plates (Scientific Laboratory Supplies, Wilford, UK). An equal volume (75 µl) of bacterial suspension was added to each well to yield a final well concentration of $5x10^5$ colony forming units (CFU)/ml. Controls were antimicrobial free and inoculum free wells. Bacterial growth was determined by measuring optical density (595 nm) of samples using a Spectramax Plus 384 microplate reader and Softmax Pro version 6.4 software (Molecular Devices, Sunnyvale, USA) immediately after inoculation and after 24 hr. incubation at 37°C. Experiments were repeated three times and replicated twice (n=6).

2.4. Literature Review

Pubmed searches for recently published papers in peer-reviewed journals containing MIC data for a range of EO components against *E. coli* and *S. aureus* that had not been tested in this study. MICs were converted to milimolar (mM) concentrations to enable comparison between studies. Where units were volumetric, densities at 25˚C according to Sigma Aldrich were used for unit conversion.

2.5. Computational Methods

Structure activity relationships (SAR) and quantitative analogues (QSAR) have long been employed to understand the links between molecular descriptors and biological activity. Indeed, the FORGE program from the Cresset Suite of molecular modelling software used in this study is the latest in a wide toolkit of structural techniques implemented to harness the relationships between activity and molecular structure.

The FORGE 3D QSAR protocols follow traditional workflow for statistical method development. Molecules begin by forming alignments with a reference or reference set, where their structures are compared to a molecule with known favourable biological activity data. These molecules are then visually inspected to ensure that alignments performed computationally are correct, before being passed onto training and test sets. These sets can originate as a single grouping of molecules containing activity data, however a partitioning is favourable in order to use the test set molecules as questioning parameters for the model developed from the training set. The training set molecules are then superimposed onto a formulated grid and a 3D QSAR model generated from the training set. The training and test set are then scored against the model and the statistical data is reported. The model is then available to visualise, and can be used for future scoring of newly-designed molecules, potential targets, or entire databases.

Within the context of this study, a 3D QSAR model has been generated from cumulated experimental data and data from literature sources. Biological activities in terms of MICs against *E. coli* and *S. aureus* have been collated and used as activity model predictors for the QSAR framework. Data from both strains were cumulated in order to obtain more generalised, unified relationships between EO components and their effect on both Gram-positive and Gram-negative bacterial strains and their growth. This enables us to consider drug targets with the broadest possible spectrum for biological activity and bacterial growth inhibition.

Once molecules were aligned to the carvacrol reference (lowest MIC), a conformational hunt was initiated in order to consider the training and test set molecules based on collective torsions and rotational degrees of freedom. The sets were aligned by substructure to carvacrol before being subject to field point analysis. Contrary to traditional QSAR methods, FORGE incorporates *field points*, as opposed to 3D-lattice intersections with probes. The advantage of considering molecular parameters in terms of field points, is that far fewer sample points are required than in lattice or grid-based techniques. These sample points are physically chosen by the software, rather than statistically derived from the model, and are therefore gauge invariant. The use of sample points provide a reliable and robust model for alignment and development of a QSAR model.

Field QSAR electrostatic parameters are generated from the set of aligned molecules and their respective field points. The electrostatic field points are extracted from these and a sphere-exclusion algorithm applied to space out the sample of field point positions, deriving a unified model for the aligned molecules. The sphere exclusion algorithm selects field points with the greatest magnitudes and negates field points within a 1Å region of each of these. The procedure is repeated for all field points until a representative set of field points covering the entire molecular surface is produced. Finally, for each of the molecules in the dataset, descriptor vectors are generated at each location at which the electrostatic field is measured. These electrostatic descriptors and the descriptor vectors are generated based on the positions of positive and negative field points for each molecule.

Steric effects are described similarly using data for heavy atoms as opposed to electrostatics. Previous studies have described evidence that for 3D QSAR techniques, Lennard-Jones/Morse potentials do not legitimately provide information to supplement simple Van der Waals volume descriptors. As such, a binary indicator variable is employed to discern probe positions either inside or outside Van der Waals radii for heavy atoms in the aligned molecules. Following this, the earlier sphere exclusion algorithm is applied in an analogous manner to that in the electrostatics field point derivation, producing an appropriate and representative set of steric field points.

Descriptors having been generated, a matrix of molecular electrostatic and volume vectors is formed. This matrix contains two substructures based on the electrostatic and volume vectors, respectively. In order to scale the descriptors, the SIMPLS algorithm is employed. Indeed, issues with the statistical validity of the model would be raised if one of the descriptor blocks exhibited a larger variance than the other. This would lead to a tendency for the regression to favour the aforementioned descriptors over the descriptor set with lower variance, regardless of the relationships to biological activity. Descriptors are therefore rescaled before running the partial least squares (PLS) analysis. Once scaling has taken place, the standard deviation of each block of descriptors becomes equal.

The SIMPLS algorithm as a regression model allows correlated descriptors to be considered. The latent variables are extracted as orthogonal components, or linear combinations of the descriptors considered in the first instance. In order to amplify the covariance between descriptors and biological

activity, the latent variables are chosen selectively, and an equation is formulated predicting activity as a linear combination of the latent variables. Implementing cross-validation through *leave one out* and *leave many out* techniques defines the best possible number of latent variables. This will by nature also correspond to the highest value of q^2 and predictive ability of the model.

From the 27 molecules with known biological activity (MIC), the dataset was partitioned to 20% test and 80% training set through a combined activity/random selection algorithm in order to robustly test the QSAR model. Carvacrol as the most potent in the training set with MIC =1.98 mM, was used as the reference and to align the training set to the compound.

3. Results, Statistics and Discussion

Carvacrol was the most antimicrobial agent tested in this study, with an MIC of 1.98 mM against both *E. coli* and *S. aureus* (Table 1). Cuminaldehyde was also strongly antimicrobial against *E. coli* but weakly antimicrobial against *S. aureus,* with MICs of 2.10 and 33.60 mM, respectively. Linalool, p-Cymene and γ-terpinene were weakly antimicrobial with MICs ranging 7.98-250.46 mM. MICs of 12 of 21 EO components obtained from literature sources were considerably lower than that of carvacrol, ranging 0.004-0.59 mM, where limonene possessed the greatest reported antimicrobial activity (Table 2). Differences in MICs observed may be attributed to susceptibility of bacterial isolates used between studies, which can vary significantly, or methodological differences as inoculum size, inoculum preparation method, growth medium and incubation time, which are known to influence MIC values [18].

The FORGE SIMPLS algorithm was used as a partial least squares regression method. The training set of 27 compounds was split into 20% test set, and 80% training set (5 and 22 compounds respectively). Stratification was established through activity. The 3D field QSAR model was calculated with the following parameters: the maximum number of PLS components was 50, with 50 Y scrambles to use; molecular weighting power was quadratically derived.

For the training and cross-validation sets, a good r^2 value of 0.807 was achieved with the model developed. A generally good distribution is observed (Fig 1a) with the training CV contributing to the few outlying points (Fig 1b). Indeed, particular molecular descriptors have been found to contribute significantly to the activities observed (Fig. 2). Ligand efficiency, calculated as a measure of average binding energy per atom, is found to correlate well to the observed activity, with an r^2 value of 0.792. The ligand efficiency was defined as 1.4(-logIC50)N where IC50 represents half the minimum inhibitory concentration, and N the number of non-hydrogen atoms.

This suggests that for future studies of EOs and their components, the ligand efficiency of the EO constituents could form an integral part of target identification. Moreover, it is possible to analyse the electrostatic origin of inhibition from activity cliff summaries. These poses are generated based on the electrostatic origin of activity, and highlight areas of positive and negative charge in the species considered (Figure 3).

Similar distributions of positive and negative charge are located in the highly potent carvacrol and menthol constituents. These are in parallel to the weakly inhibitory terpinen-4-ol and 1,8-cineole EO components, which demonstrate low biological activity, however, both lack the region of strong negative electrostatics present in the highly potent molecules of carvacrol and menthol.

An important concept in terms of activity cliffs and summaries is that of disparity and associated matrices. The activity miner employed here uses a combination of 3D and 2D molecular similarity parameters in order to find regions or structure activity relationships which are particularly influential in a chemical structure or moiety. The disparity between a pair of molecules can be defined as the difference in their activity as a quotient of their distance. Disparity effectively measured the difference in activity based on substructure. A pair of molecules with a high disparity index indicates that the molecular structures are likely similar, however the activities differ significantly. This helps to identify structural features inherently important in the biological activity of a set of molecules.

The disparity matrix (Table 3) highlights certain structural features incorporated in the compounds tested, which affect the biological activity in situ. Indeed, compounds such as α-pinene and 1,8-

cineole possess little similarity bar the presence of cyclic alkyl, contributing to steric bulk of the compound. Moreover, this feature is also highlighted in carvacrol and menthol, both of these also featuring prominently in the pair matching of the disparity matrix.

4. Conclusions

The QSAR study on antimicrobial effects of essential oil components provides some promising targets for identification and future bacterial screening . Indeed, the steric effects of some EO components have been shown as a structural commonality between inhibitory molecules, with the electrostatic properties and topography correlating well with the lowest MICs. Carvacrol and menthol were found to have the lowest MICs against *E. coli* and *S. aureus*, with highly correlated electrostatic topographies. Most notably, the ligand efficiency, defined as a function of the MIC and the number of heavy (non-hydrogen atoms), has been noted to correlate well with EO components exhibiting high antimicrobial activity. This is a promising finding which will help lead target identification for future studies of essential oils, their components, and the use of natural products in antimicrobial treatments.

Acknowledgements: This research did not receive any specific grant from funding agencies in the public, commercial, or not-for-profit sectors.

Conflicts of interest: none.

References

[1] Laxminarayan, R., Matsoso, P., Pant, S., Brower, C., Røttingen, J.-A., Klugman, K., Davies, S., 2016. Access to effective antimicrobials: a worldwide challenge. Lancet 387, 168–175.

[2] Laxminarayan, R., Duse, A., Wattal, C., Zaidi, A.K.M., Wertheim, H.F.L., Sumpradit, N., Vlieghe, E., Hara, G.L., Gould, I.M., Goossens, H., Greko, C., So, A.D., Bigdeli, M., Tomson, G., Woodhouse, W., Ombaka, E., Peralta, A.Q., Qamar, F.N., Mir, F., Kariuki, S., Bhutta, Z.A., Coates,

A., Bergstrom, R., Wright, G.D., Brown, E.D., Cars, O., 2013. Antibiotic resistance-the need for global solutions. Lancet Infect. Dis. 13, 1057–1098.

[3] Pandey, A.K., Kumar, P., Singh, P., Tripathi, N.N., Bajpai, V.K., 2017. Essential oils: sources of antimicrobials and food preservatives. Front. Microbiol. 7, https://dx.doi.org/10.3389/fmicb.2016.02161

[4] Raut, J.S., Karuppayil, S.M., 2014. A status review on the medicinal properties of essential oils. Ind. Crops Prod. 62, 250–264.

[5] Rehman, R., Hanif, M.A., Mushtaq, Z., Al-Sadi, A.M., 2016. Biosynthesis of essential oils in aromatic plants: A review. Food Rev. Int. 32, 117–160.

[6] Dudareva, N., Klempien, A., Muhlemann, J.K., Kaplan, I., 2013. Biosynthesis, function and metabolic engineering of plant volatile organic compounds. New Phytol. 198, 16–32.

[7] Sokovic, M., Marin, P.D., Brkic, D., Griensven, L.J.L.D. van, 2008. Chemical composition and antibacterial activity of essential oils against human pathogenic bacteria. Food 1, 220–226.

[8] Hammer, K.A., Carson, C.F., Riley, T.V., 2012. Effects of *Melaleuca alternifolia* (tea tree) essential oil and the major monoterpene component terpinen-4-ol on the development of single- and multistep antibiotic resistance and antimicrobial susceptibility. Antimicrob. Agents Chemother. 56, 909-915.

[9] Wang, T.-H., Hsia, S.-M., Wu, C.-H., Ko, S.-Y., Chen, M.Y., Shih, Y.-H., Shieh, T.-M., Chuang, L.C., Wu, C.-Y., 2016. Evaluation of the antibacterial potential of liquid and vapor phase phenolic essential oil compounds against oral microorganisms. PLoS One 11, http:/dx.doi.org/10.1371/journal.pone.0163147

[10] Orhan, I.E., Ozcelik, B., Kan, Y., Kartal, M., 2011. Inhibitory effects of various essential oils and individual components against extended-spectrum beta-lactamase (ESBL) produced by *Klebsiella pneumoniae* and their chemical compositions. J. Food Sci. 76, 538–546.

[11] Nazzaro, F., Fratianni, F., De Martino, L., Coppola, R., De Feo, V., 2013. Effect of essential oils on pathogenic bacteria. Pharmaceuticals (Basel) 6, 1451–1474.

[12] Langeveld, W.T., Veldhuizen, E.J.A., Burt, S.A., 2014. Synergy between essential oil components and antibiotics: a review. Crit. Rev. Microbiol. 40, 76–94.

[13] Hurdle, J.G., O'Neill, A.J., Chopra, I., Lee, R.E., 2011. Targeting bacterial membrane function: an underexploited mechanism for treating persistent infections. Nat. Rev. Microbiol. 9, 62–75.

[14] Andrade-Ochoa, S., Nevárez-Moorillón, G.V., Sánchez-Torres, L.E., Villanueva-García, M., Sánchez-Ramírez, B.E., Rodríguez-Valdez, L.M., Rivera-Chavira, B.E., 2015. Quantitative structure-activity relationship of molecules constituent of different essential oils with antimycobacterial activity against *Mycobacterium tuberculosis* and *Mycobacterium bovis*. BMC Complement. Altern. Med. 15, 332.

[15] Ben Arfa, A., Combes, S., Preziosi-Belloy, L., Gontard, N., Chalier, P., 2006. Antimicrobial activity of carvacrol related to its chemical structure. Lett. Appl. Microbiol. 43, 149–154.

[16] Ultee, A., Bennik, M.H.J., Moezelaar, R., 2002. The phenolic hydroxyl group of carvacrol is essential for action against the food-borne pathogen *Bacillus cereus*. Appl. Environ. Microbiol. 68, 1561–1568.

[17] Veldhuizen, E.J.A., Tjeerdsma-van Bokhoven, J.L.M., Zweijtzer, C., Burt, S.A., Haagsman, H.P., 2006. Structural requirements for the antimicrobial activity of carvacrol. J. Agric. Food Chem. 54, 1874–1879.

[18] ISO, ISO 20776-1: Clinical laboratory testing and in vitro diagnostic test systems — Susceptibility testing of infectious agents and evaluation of performance of antimicrobial susceptibility test devices — Part 1: Reference method for testing the in vitro activity of antimicrobial agents against rapidly growing aerobic bacteria involved in infectious diseases. ISO, Geneva, 2006.

[19] Balouiri, M., Sadiki, M., Ibnsouda, S.K., 2016. Methods for in vitro evaluating antimicrobial activity: A review. Journal of Pharmaceutical Analysis 6, 71–79.

[20] Rosato, A., Vitali, C., De Laurentis, N., Armenise, D., Antonietta Milillo, M., 2007. Antibacterial effect of some essential oils administered alone or in combination with norfloxacin. Phytomedicine 14, 727–732.

[21] Chan, A.C., Ager, D., Thompson, I.P., 2013. Resolving the mechanism of bacterial inhibition by plant secondary metabolites employing a combination of whole-cell biosensors. J. Microbiol. Methods 93, 209–217.

[22] Zengin, H., Baysal, A.H., 2014. Antibacterial and antioxidant activity of essential oil terpenes against pathogenic and spoilage-forming bacteria and cell structure-activity relationships evaluated by SEM microscopy. Molecules 19, 17773–17798.

[23] Jirovetz, L., Buchbauer, G., Denkova, Z., Slavchev, A., Stoyanova, A. and Schmidt, E., 2006. Chemical composition, antimicrobial activities and odor descriptions of various *Salvia* sp. and *Thuja* sp. essential oils. Nutrition, 30, 152.

[24] Knight, K.P., McKellar, R.C., 2007. Influence of cinnamon and clove essential oils on the D- and Z-values of *Escherichia coli* O157:H7 in apple cider. J. Food Prot. 70, 2089–2094.

[25] Gallucci, M.N., Oliva, M., Casero, C., Dambolena, J., Luna, A., Zygadlo, J., Demo, M., 2009. Antimicrobial combined action of terpenes against the food-borne microorganisms *Escherichia coli, Staphylococcus aureus* and *Bacillus cereus*. Flavour Fragr. J. 24, 348–354.

[26] Adukwu, E.C., Bowles, M., Edwards-Jones, V., Bone, H., 2016. Antimicrobial activity, cytotoxicity and chemical analysis of lemongrass essential oil (*Cymbopogon flexuosus*) and pure citral. Appl. Microbiol. Biotechnol. 100, 9619–9627.

Figure 1

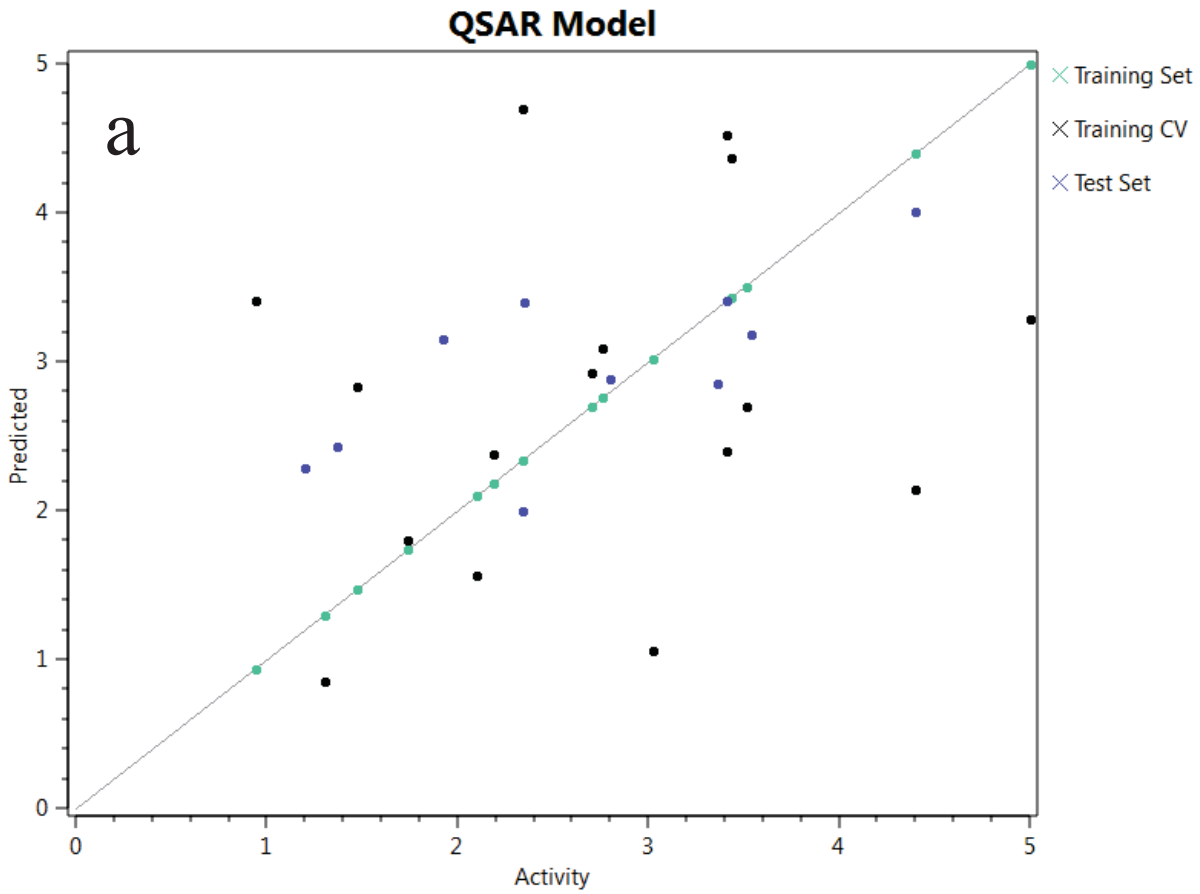
QSAR Model
a
Training Set
Training CV
Test Set
Predicted
Activity
0
1
2
3
4
5

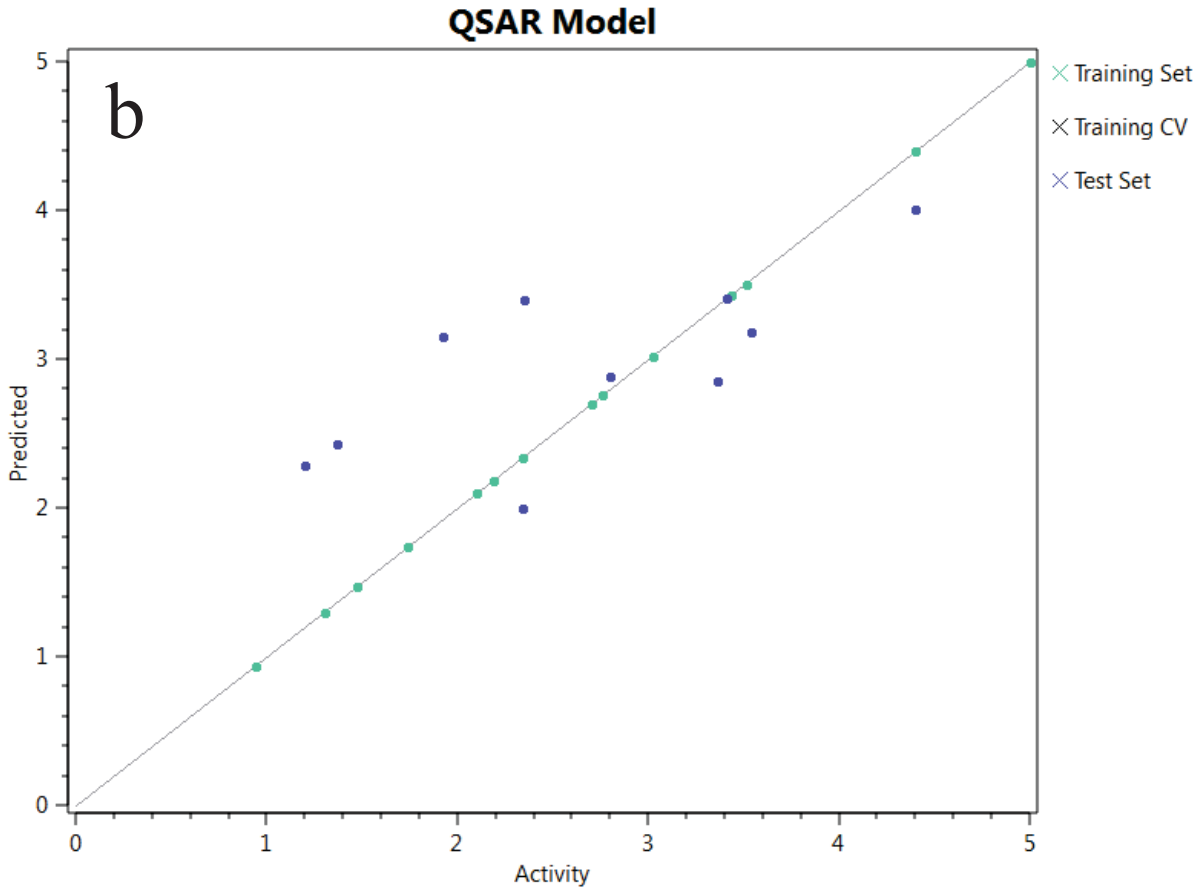

Figure 1(a) and (b). Three-component EO 3D-QSAR model – predicted against experimental activity of compounds in the training and test sets.

Figure 2

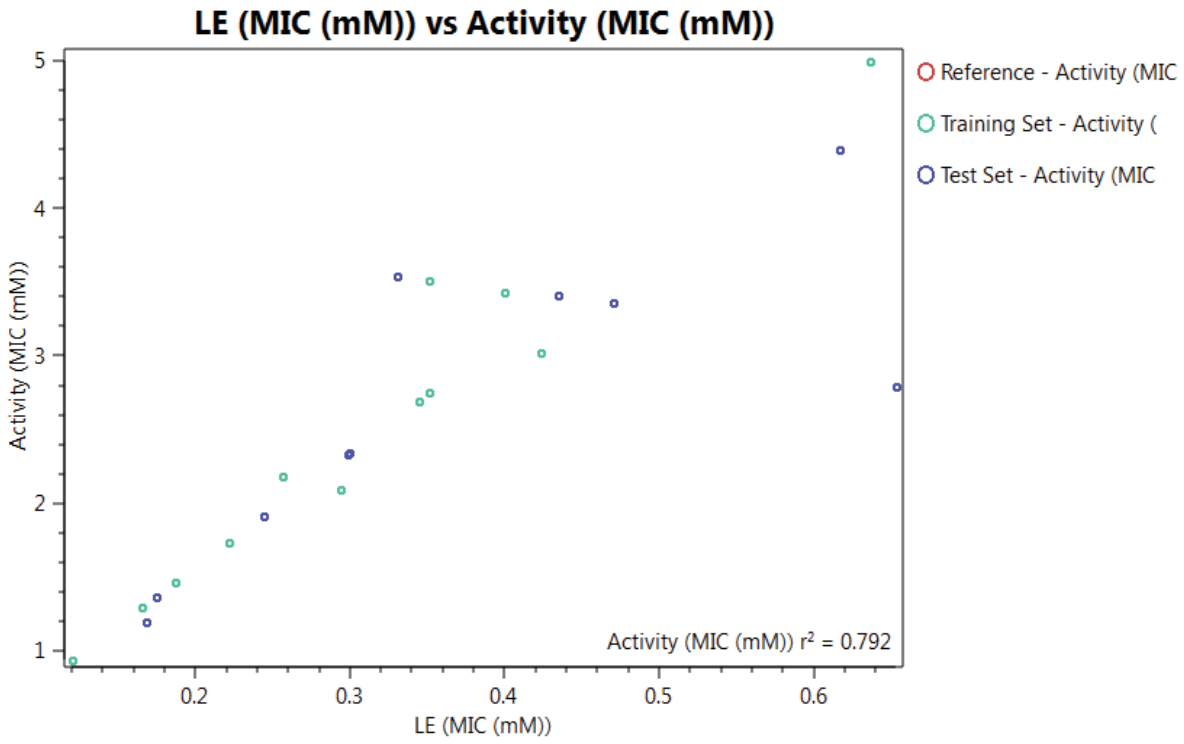

Figure 2. Ligand efficiency relation to activity observed, showing good agreement with the QSAR model developed.

Figure 3

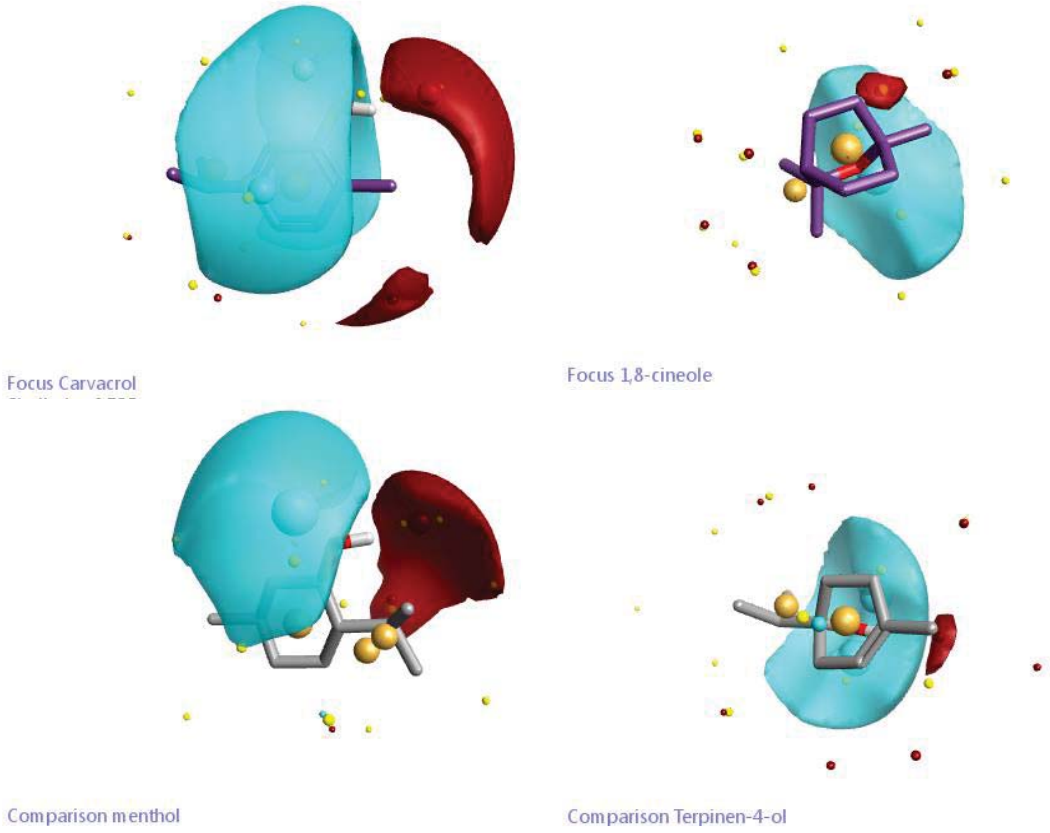

Figure 3. Comparison of electrostatic field points for highly potent (carvacrol and menthol) and weakly inhibitory (1,8-cineole and terpinen-4-ol) EO components. Activity cliffs in the form of positive (red) charge and negative (blue) charge areas are shown.

Table 1

Table 1: MIC (mM) of EO components against *E. coli* and *S. aureus* (n=6).

EO component	MIC (mM)	
	E. coli	***S. aureus***
Carvacrol	1.98	1.98
Cuminaldehyde	2.10	33.60
Linalool	57.05	114.10
p-Cymene	15.97	7.98
γ-Terpinene	250.46	62.61

Table 2: MIC (mM) of EO components against *E. coli* and *S. aureus* from the published literature sources.

EO Component	MIC (mM)		Reference
	E. coli	*S. aureus*	
1,8-cineole	18.15	18.15	[20]
Allyl isothiocyanate	1.58	1.58	[21]
α-pinene	0.06	0.04	[7]
α-Terpineol	36.18	42.20	[22]
α-thujone	0.39	0.39	[23]
β-Caryophyllene	0.29	0.29	[23]
β-pinene	0.06	0.04	[7]
β-Thujone	0.04	0.39	[23]
Camphor	0.05	0.39	[7,23]
Carvone	6.38	50.19	[24,25]
Cinnamaldehyde	0.59	0.95	[8,21]
Citral		1.75	[26]
Citronellol	8.95	4.48	[20]
Eugenol		6.50	[8]
Geraniol	9.08	4.54	[20]

Hinokitiol	0.24		[22]
Limonene	0.004	0.44	[23]
Linalyl acetate	0.05	0.31	[7,23]
Menthol	0.01	0.01	[7]
Terpinen-4-ol	0.04	12.10	[8,23]
Thymol	9.32	4.60	[20]

Table 3. Disparity Matrix for EO components based on activity and structural information. Green indicates a high disparity, yellow little disparity, and red, significant disparity.

	A	B	C	D	E	F	G	H	I	J	K	L	M	N	O	P	Q	R	S	T	U	V	W	X	Y
A	0	0	-8.4	0	3.9	-1.9	0	6.8	2.4	-3	1.3	0	3	0	5.4	3.2	4.4	-2.6	-1.4	-2.9	0.9	2.2	2.5	1.9	-1.7
B	0	0	-11.8	5.7	5	0	0	8.1	2.8	-2.4	2.1	0	3.8	0	6.6	4.1	5.3	-2	0	-2.4	1.6	2.6	3.1	2.4	-1.3
C	8.4	11.8	0	13.6	8.9	3.2	3.5	9.4	5.3	0	5.3	3.2	7	2.4	8.4	5.8	7.5	0	1.2	0	3.5	4	4.8	3.9	0
D	0	-5.7	-13.6	0	4.1	-3.2	-2.4	8.7	0	-3.8	0	0	1.9	0	5.1	2.2	4.2	-3.5	-2.3	-4.5	0	1.6	1.7	1.2	-2.3
E	-3.9	-5	-8.9	-4.1	0	-4.1	-3.5	4.2	-0.9	-4.6	-1.4	-2.5	0	-2.4	2.3	0	2.3	-3.9	-3.4	-6.3	-1.2	0	0	0	-3.6
F	1.9	0	-3.2	3.2	4.1	0	0	8.1	3	-1.5	2.2	0.9	3.1	0.9	5.9	3.8	5.3	-1.5	0	-2.1	1.8	2.8	3.4	2.7	-0.8
G	0	0	-3.5	2.4	3.5	0	0	6.6	2.5	-1.9	1.5	0	2.6	0	5.1	3.6	4.9	-1.8	-1	-2.5	1.1	2.3	2.6	2.3	-1.3
H	-6.8	-8.1	-9.4	-8.7	-4.2	-8.1	-6.6	0	-4.4	-8.2	-4.4	-6.5	-2.6	-8.6	-1.6	-3.2	-1.2	-7	-6.3	-8.1	-5	-3.7	-3.4	-2.7	-7.1
I	-2.4	-2.8	-5.3	0	0.9	-3	-2.5	4.4	0	-3.5	0	-1.8	0	-1.3	3	1.2	2.8	-3.8	-3	-4.8	0	0	1	0	-2.6
J	3	2.4	0	3.8	4.6	1.5	1.9	8.2	3.5	0	3.2	1.8	3.5	2.1	6.5	4.4	5.9	0	0	-0.8	2.6	3.7	4.3	3.8	0
K	-1.3	-2.1	-5.3	0	1.4	-2.2	-1.5	4.4	0	-3.2	0	-1.1	1.2	-0.9	3.3	1.5	3.1	-3.2	-2.3	-3.8	0	1	1.4	1.1	-2.3
L	0	0	-3.2	0	2.5	-0.9	0	6.5	1.8	-1.8	1.1	0	2	0	4.2	2.5	4	-1.9	-1.1	-3.5	0.8	1.9	2	1.6	-1.3
M	-3	-3.8	-7	-1.9	0	-3.1	-2.6	2.6	0	-3.5	-1.2	-2	0	-1.6	2	0	1.9	-3.5	-2.6	-5	-1	0	0	0	-2.6
N	0	0	-2.4	0	2.4	-0.9	0	8.6	1.3	-2.1	0.9	0	1.6	0	4.4	2.4	4	-2	-1.4	-2.9	1	2.1	2.6	1.9	-1.6
O	-5.4	-6.6	-8.4	-5.1	-2.3	-5.9	-5.1	1.6	-3	-6.5	-3.3	-4.2	-2	-4.4	0	-1.7	0	-6.4	-5.7	-6.5	-3.2	-1.9	-1.7	-1.9	-5.1
P	-3.2	-4.1	-5.8	-2.2	0	-3.8	-3.6	3.2	-1.2	-4.4	-1.5	-2.5	0	-2.4	1.7	0	1.7	-4.3	-3.7	-4.7	-1.5	0	0	0	-3.7
Q	-4.4	-5.3	-7.5	-4.2	-2.3	-5.3	-4.9	1.2	-2.8	-5.9	-3.1	-4	-1.9	-4	0	-1.7	0	-5.5	-5.7	-6.5	-2.9	-1.8	-1.5	-1.8	-5
R	2.6	2	0	3.5	3.9	1.5	1.8	7	3.8	0	3.2	1.9	3.5	2	6.4	4.3	5.5	0	1.1	0	3.1	3.3	4.6	4.3	0
S	1.4	0	-1.2	2.3	3.4	0	1	6.3	3	0	2.3	1.1	2.6	1.4	5.7	3.7	5.7	-1.1	0	-1.6	2.3	2.8	3.6	3.6	0
T	2.9	2.4	0	4.5	6.3	2.1	2.5	8.1	4.8	0.8	3.8	3.5	5	2.9	6.5	4.7	6.5	0	1.6	0	3	4	4.7	3.6	0.9
U	-0.9	-1.6	-3.5	0	1.2	-1.8	-1.1	5	0	-2.6	0	-0.8	1	-1	3.2	1.5	2.9	-3.1	-2.3	-3	0	1.2	1.7	1.4	-2.3
V	-2.2	-2.6	-4	-1.6	0	-2.8	-2.3	3.7	0	-3.7	-1	-1.9	0	-2.1	1.9	0	1.8	-3.3	-2.8	-4	-1.2	0	0	0	-3.2
W	-2.5	-3.1	-4.8	-1.7	0	-3.4	-2.6	3.4	-1	-4.3	-1.4	-2	0	-2.6	1.7	0	1.5	-4.6	-3.6	-4.7	-1.7	0	0	0	-3.7
X	-1.9	-2.4	-3.9	-1.2	0	-2.7	-2.3	2.7	0	-3.8	-1.1	-1.6	0	-1.9	1.9	0	1.8	-4.3	-3.6	-3.6	-1.4	0	0	0	-3.4
Y	1.7	1.3	0	2.3	3.6	0.8	1.3	7.1	2.6	0	2.3	1.3	2.6	1.6	5.1	3.7	5	0	0	-0.9	2.3	3.2	3.7	3.4	0

Table 4. Molecular identities used to describe compounds in Table 3.

ID	Compound
A	Thymol
B	p-Cymene
C	γ-Terpinene
D	Carvacrol
E	Hinokitiol
F	Terpinen-4-ol
G	Eugenol
H	menthol
I	Cinnamaldehyde
J	α-Terpineol
K	Allyl isothiocyanate
L	Geraniol
M	limonene
N	Citronellol
O	α-pinene
P	β-caryophyllene
Q	β-pinene
R	Carvone
S	1,8-cineole
T	Linalool
U	Citral
V	α-thujone
W	linalyl acetate
X	Camphor
Y	Cuminaldehyde